EFFECT OF VIBRATION ON YIELD STRESS OF CONCRETE FOR 3D PRINTING APPLICATIONS

BY

KARTHIK PATTAJE SOORYANARAYANA

THESIS

Submitted in partial fulfillment of the requirements
for the degree of Master of Science in Civil Engineering
in the Graduate College of the
University of Illinois at Urbana-Champaign, 2018

Urbana, Illinois

Adviser:

Professor David A. Lange

ABSTRACT

Concrete 3D printing is one of the latest developments in the field of construction. It promises several benefits but needs further development before it can be used as a practical construction technique. One primary challenge is the requirement for 3D printable concrete to behave like a fluid during pumping and extrusion, and like a solid after extrusion. This paradox could potentially be solved by using vibration to control the yield stress of concrete. Research has shown that concrete behaves like a Newtonian fluid during vibration at low shear rates. The primary objective of this research is to qualitatively understand the effects of vibration on the fresh properties of concrete and its implications for 3D printing with a vibrating nozzle.

An existing concrete rheometer was modified to be able to reliably measure yield stress of concrete during vibration. This thesis details the modifications made to the rheometer and discusses the reliability of the measurements made with the modified rheometer. The relationship between yield stress and time was evaluated and the effect of the destructive yield stress measurement technique on its result was discussed.

A test protocol was developed to mimic concrete 3D printing using vibration. The parabolic relationship between yield stress and sand content was verified at different hydration ages using the developed test protocol. The effect of vibration on the yield stress of concrete during the dormant stage was studied. The reduction in yield stress during vibration was found to be instantaneous and reversible throughout the dormant period. It was also found out that vibration causes the yield stress of concrete to grow at a slower pace. It was also observed that the effect of vibration on concrete is dependent on the amplitude of vibration.

ACKNOWLEDGMENTS

I would like to thank my adviser Prof. David Lange for his guidance and support throughout the course of my research. I would also like to acknowledge and thank Dr. Peter Stynoski for his constant support and advise, and for providing the funding for this research project through the US Army ERDC-CERL (applied research project titled 'Advanced Materials for Advanced Manufacturing'). I am also grateful to Kathleen Hawkins for being a wonderful partner in this research project.

I want to thank Lillian Lau, Benjamin Tung, and Dev Desai for being patient and helpful undergraduate research assistants. I am thankful to Jamar Brown and Tim Prunkard for their assistance in the laboratory. I also appreciate my fellow graduate research assistants for their friendship, advise and company.

Finally, this work was made easier with the constant support of my friends and family. I am grateful for my ever-supporting parents for all the confidence they have in me.

TABLE OF CONTENTS

CHAPTER 1: INTRODUCTION

One of the recent developments in the field of construction is using 3D printing (3DP) technology to build structures. Automation in construction using 3DP promises several benefits like formwork free construction, architectural freedom/customization, safer construction environment (reduced construction accidents involving laborers), better quality control in construction, and more efficiency in construction [1][2][3].

Currently, 3DP with cementitious material generally involves extruding cement paste/mortar from a nozzle or deposition head (Figure 1) which is mounted on a gantry, robot arm or a crane as shown in Figures 2, 3, and 4 [4]. The deposition head or nozzle deposits the cementitious material layer after layer to 'print' the structure. The position of the deposition head is controlled by a computer which can dictate the coordinates in the 3-dimensional space.

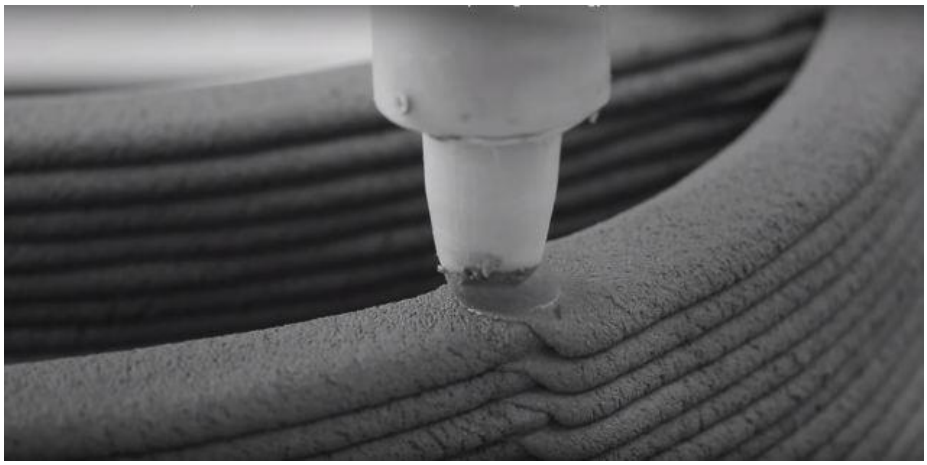

Figure 1: Cementitious material being extruded during 3DP [5].

Figure 2: 3DP using a gantry system [6].

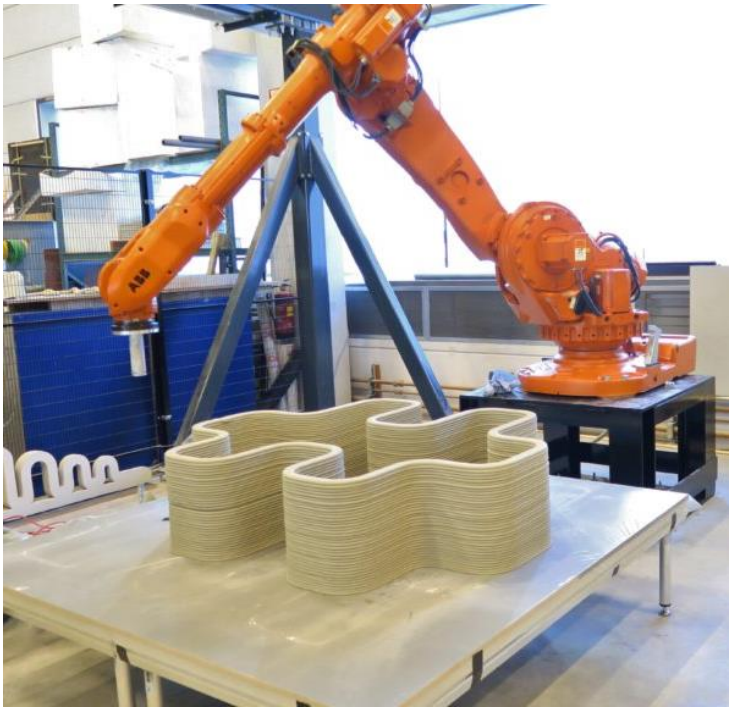

Figure 3: 3DP using a robot arm [7].

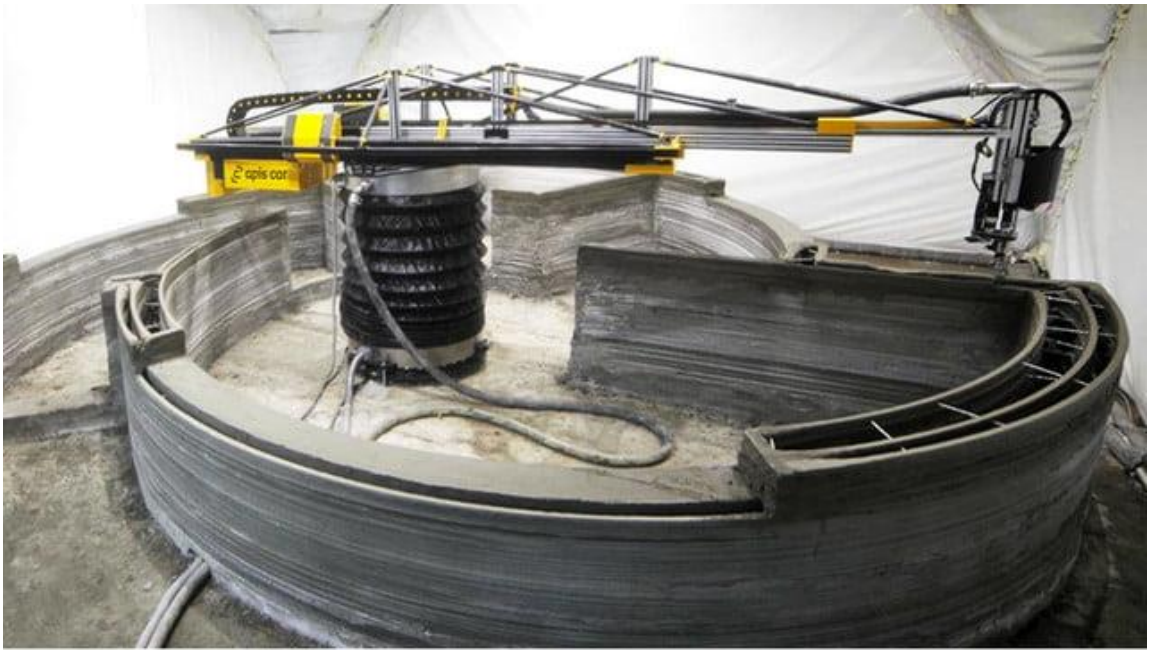

Figure 4: 3DP using a crane [8].

Along with its numerous benefits, construction with 3DP has a few drawbacks. Currently, coarse aggregates are avoided in concrete 3DP as it clogs the extruder [1]. This is one of the reasons for the 3DP community to largely use cement paste and/or mortar for printing structures. This prevents the printing of load-bearing structures. A printed layer needs to be load bearing before it can receive the next printed layer (else run the risk of losing its shape); the strength gain from cement maturity is required to outpace the load accumulation from the subsequent layers being printed [2]. To address this issue, researchers have used many tailor-made mixture designs that have included using accelerating admixtures to reduce the setting time, including fibers to increase the yield stress, and using viscosity modifiers to control viscosity [2] [9] [10] [11] [12] [13]. Research has also been carried out to investigate if longer stoppage time between layer printing or applying heat to accelerate the cement hydration process can help with stabilizing the shape of the printed layers [14]. The stoppage time between layers leads to another drawback of extrusion-based concrete

3DP, decreased bond strength between layers [15]. Shrinkage is also a common issue faced during concrete 3DP. The lack of formwork causes a large surface area to be exposed to the air [12]. The lack of aggregates and high cement content in these mixture designs further compounds this problem. The need for tailor-made materials acts as a setback in the adoption of this technology by the construction industry due to lack of technological know-how and high costs. Some research has been carried out in using conventional concrete mixture designs to print large scale structures which incorporate coarse aggregate and commonly available materials [1].

Addressing the paradox of requiring a high yield stress to resist loading but a low yield stress while being extruded has been one of the focuses of the concrete 3DP community. This has mostly been addressed by manipulating the concrete mixture design as previously mentioned. The actual process of material deposition has remained unchanged and extrusion remains the most popular choice for concrete 3DP.

Various researchers have shown that stiff concrete behaves like a Newtonian fluid at low shear rates under vibration [16][17][18][19]. Using this idea, in this research project, a new method for concrete 3DP is proposed which incorporates a vibrating nozzle to control material deposition. A schematic of the proposed idea is shown in Figure 5. Using a no-slump concrete, with its inherent high yield stress should help solve the problem of layer shape stability under loading at early ages. Concrete with no slump can be used in concrete 3DP if it can be successfully allowed to flow out of the printer. The effect of vibration on the yield stress of concrete has been found to be instantaneous and reversible [16]. This research project aims to use concrete with no special additives to help promote easy adoption by the construction industry. By using coarser aggregates, the printed concrete is expected to be cost-effective due to the lower cement content, have better shrinkage resistance and in general have a longer life because of the better durability of concrete

over cement paste/mortar [20]. The end goal of this research is to be able to print structural concrete members/structures.

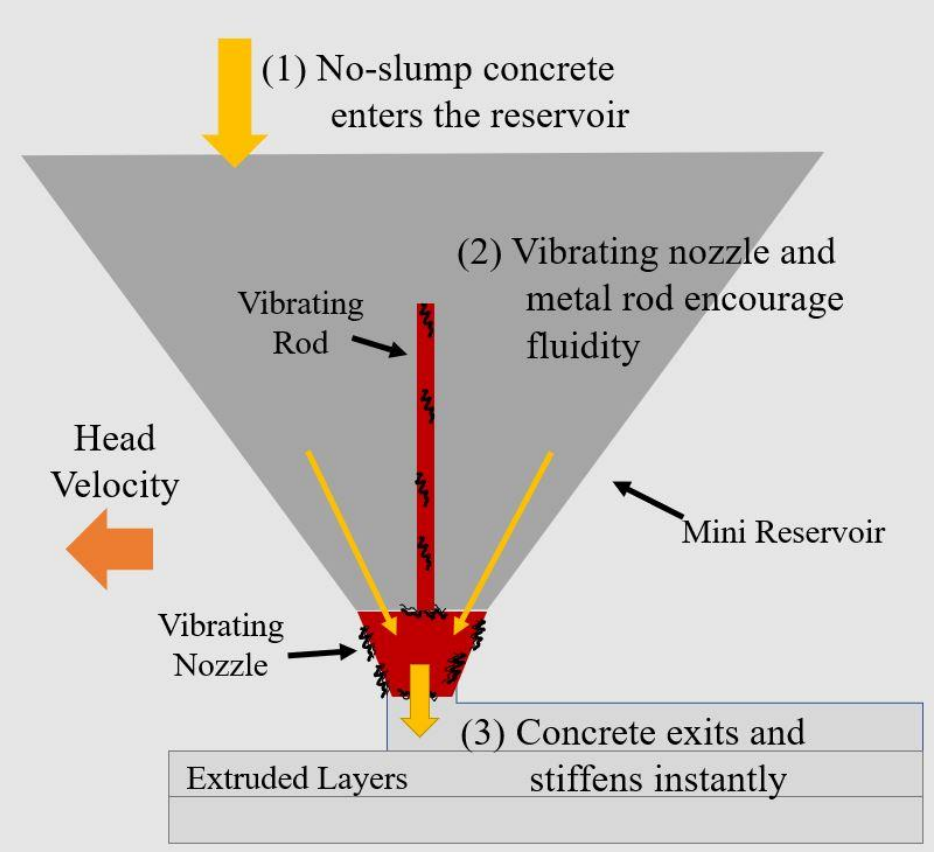

Figure 5: Schematic of the proposed 3DP extruder.

The primary objective of this project is to qualitatively understand the behavior of concrete (in terms of its yield stress) before, during, and after vibration. The changes in this response over time were also investigated. This project was intended to be a proof of concept study in preparation towards a larger goal of concrete 3DP using a vibrating nozzle.

This thesis contains 4 more chapters; chapter 2 presents a review of the current literature relevant to this research project, chapter 3 details the materials and experimental methods used, chapter 4 presents and discusses the results obtained, and conclusions are made in chapter 5.

CHAPTER 2: LITERATURE REVIEW

2.1 Concrete Rheology

The term rheology has been defined as the science of deformation and flow of matter under the influence of stresses [21]. Rheology of concrete affects how it is handled at early age. The effort required to mix, handle, transport, cast, consolidate, and finish depends on the rheology of concrete. Traditionally, the qualitative term 'workability' has been used to describe the ease of handling concrete. The workability of concrete is measured by the slump test of concrete (ASTM C143) [22]. The slump test of concrete is a low shear rate flow simulation of concrete flow and gives a direct indication of its yield stress [23].

Concrete is a composite material that can be described as a suspension of coarse aggregate in mortar matrix. The mortar matrix, in turn, is a suspension of sand in cement paste. In multiphase fluids, yield stress occurs commonly (for e.g., concentrated suspensions). The solid phase flocculates and forms a skeletal structure which resists flow at low stresses. The stress which needs to be overcome to initiate the flow is related to the force required to break down the skeletal structure formed and is termed yield stress [24].

Figure 6 illustrates different rheological behaviors. Concrete has traditionally been modeled as a Bingham fluid, expressed as

$$\tau = \tau_o + \mu_p \dot{\gamma} \quad (1)$$

where,

τ is the shear stress (Pa);

τ_o is the yield stress (Pa);

μ_p is the plastic viscosity (Pa.s); and

$\dot{\gamma}$ is the shear rate (s^{-1}).

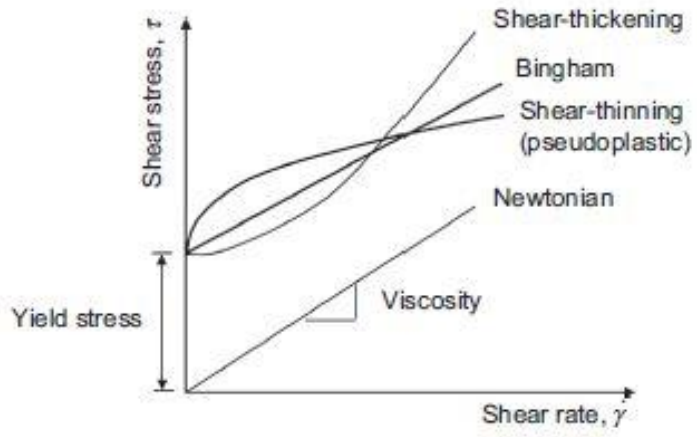

Figure 6: Illustration of various rheological behaviors [21].

Thixotropy is defined as the breakdown of the structure under shear and rebuilding at rest. A thixotropic material undergoes a reversible, time-dependent decrease in viscosity when subjected to constant shearing. In cementitious material, thixotropy exists along with structural breakdown which is irreversible. Thixotropy is time-dependent and hence the shear history of a thixotropic material is important.

To measure thixotropy, a destructive test is carried out where the rate at which structural build-up takes place at rest is measured. Since cement is also chemically reactive, to limit the modification of the system by hydration reaction, multiple samples are prepared and measured at different times [21].

Static yield stress is the minimum stress required to initiate flow from rest and dynamic yield stress is the minimum stress required for maintaining the flow. The measurement of static yield stress which is also referred to as the shear-growth yield stress involves subjecting the sample to low stress at a constant rotational speed in the rheometer. The resistance of the rheometer to maintain a constant speed (rheometers record this value as torque) is plotted against time. The maximum torque recorded corresponds to the yield stress of the sample.

The mixture design of concrete has a significant impact on its rheology. Figure 7 presents an illustration which describes the influence of various ingredients of paste on the rheology of concrete. Figure 8 presents an illustration which describes the influence of aggregate shape and content on the rheology of concrete.

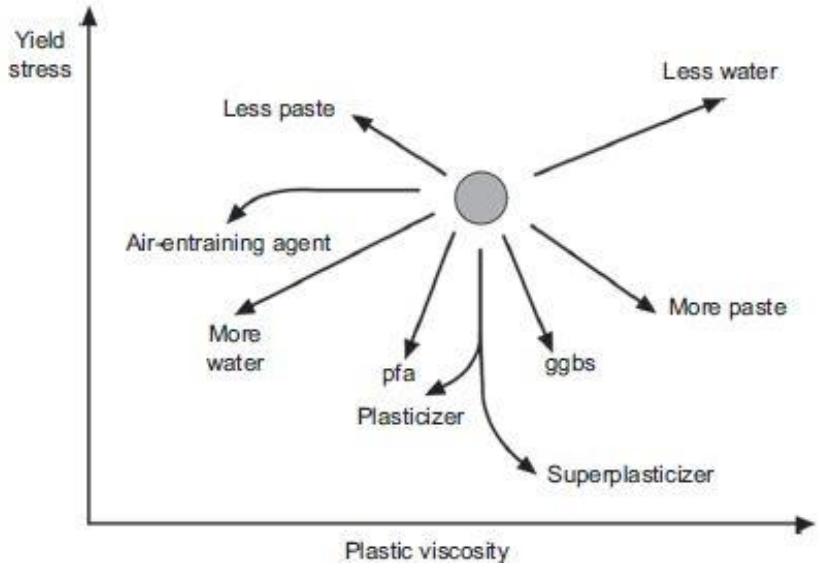

Figure 7: Illustration of various ingredients of paste on its rheology [25].

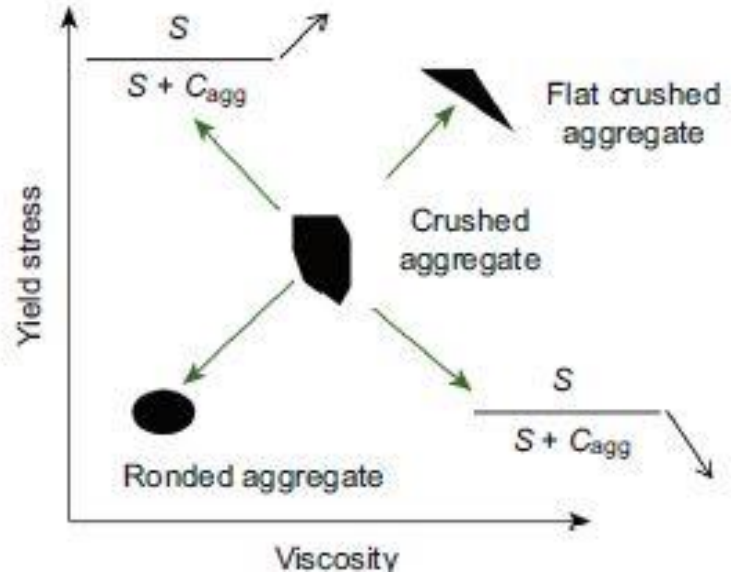

Figure 8: Effect of aggregate shape and content on concrete rheology (S – sand & C_{agg} – coarse aggregate) [21] [26].

However, in other research, it has been found that the yield stress of concrete has a parabolic relationship with sand content [27]. The yield stress of concrete was found to have a minimum value at around 35% to 40% regardless of the coarse aggregate shape as can be seen in Figure 9. The viscosity of concrete was also found to be minimum at this intermediate sand content. The author relates this to the maximum volume fraction, which occurs at about the same intermediate sand content as can be seen in Figure 10. The same study also found that the yield stress of concrete increased with an increase in aggregate volume and the viscosity of the concrete increased with an increase in the aggregate volume concentration [27]. And, the yield stress decreased with increase in the water-to-cement ratio.

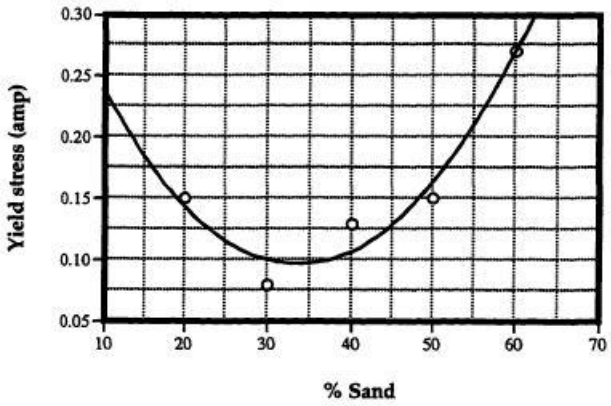

Figure 9: Relationship between % sand (of total aggregate by volume) and yield stress [27].

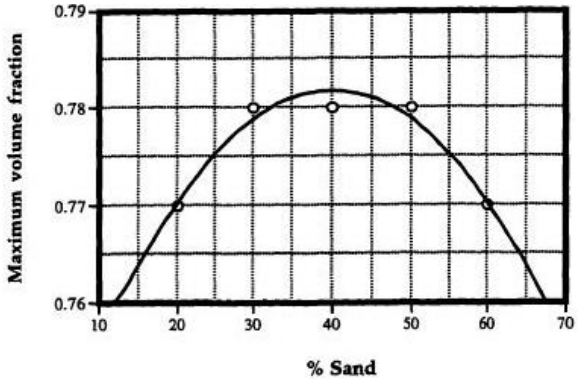

Figure 10: Relationship between % sand (of total aggregate by volume) and maximum volume fraction [27].

2.2 Effect of Vibration on Concrete Rheology

It is not easy to measure rheological parameters during vibration [28]. One of the commonly used methods is to place the concrete rheometer on a vibration table and to run the rheometer with the vibration table turned on [17] [18] [19] [28]. The effect of vibration on concrete has been found to be instantaneous and reversible [16]. It was observed that the drop in torque because of vibration was recovered immediately when the vibration was turned off and the torque was found to return

to its original value [16]. Concrete has been found to behave like a Newtonian fluid at low shear rates with the yield stress of concrete tending to a zero value [16] [17] [19]. Under vibration, concrete does not show a Bingham behavior and this behavior of concrete has been defined by various researchers as a power law pseudoplastic fluid with zero yield stress and as a quasi-viscous flow [16] [28]. The reasoning given for this behavior is that vibration reduces the shear resistance of the system. The cement paste forms a viscous layer around the aggregates, reducing friction since the aggregates are no longer in direct contact [17]. It was found that the effect of vibration is greater as the particle size increases and vibration has no effect on cement paste as its size is too small [17].

It has also been observed that vibration has no effect on concrete rheology below a certain threshold amplitude and above a certain limiting frequency [18]. The threshold amplitude was found to be dependent on the frequency of the vibration and the limiting frequency was dependent on the maximum aggregate size [18]. The maximum velocity of the vibration was the key parameter in assessing the effect of vibration on concrete [18]. Further, it has been observed that frequencies below 300 Hz are the most efficient in reducing the shear resistance of cementitious systems [28].

CHAPTER 3: MATERIALS AND EXPERIMENTAL PROCEDURES

The experimental work in this project was carried out to qualitatively study the effects of vibration on concrete. The focus was mainly on modifying the existing concrete rheometer to measure yield stress during vibration effectively. Experiments were designed and carried out to replicate results seen in literature.

3.1 Materials

The cement used in this study was a Type I/II ordinary Portland cement conforming to ASTM C 150 [29]. The fine aggregate used was natural sand and the coarse aggregate was crushed limestone, both locally sourced. The aggregates were characterized according to relevant standards, ASTM C 127 and ASTM C 128, and the results are tabulated in Table 1 [30] [31]. The sieve analysis of the aggregates was carried out according to ASTM C136 and the results are shown in Figure 11 [32].

Table 1: Specific gravity and water absorption of aggregates

Property	Natural Sand	Crushed Limestone
Specific Gravity (SSD)	2.59	2.64
Specific Gravity (OD)	2.55	2.54
Absorption (%)	1.8	3.4

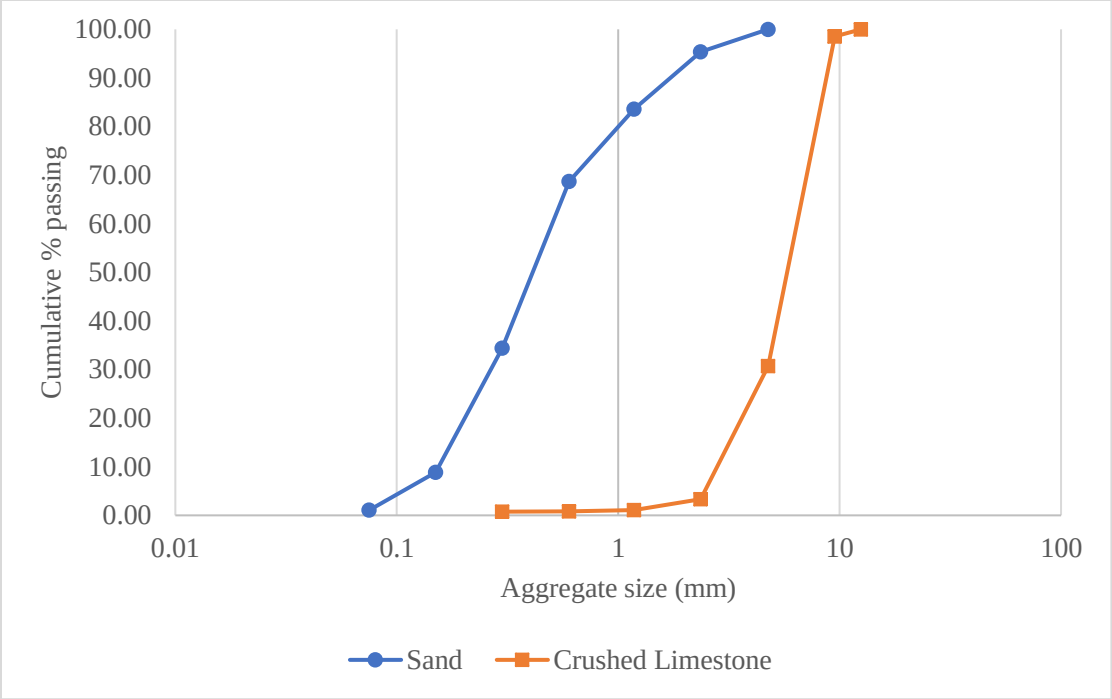

Figure 11: Results of sieve analysis.

3.2 Concrete Mixture Design

The concrete was designed based on absolute volume concept. The volume of paste (V_p) was considered as 35% of the total concrete volume. The volume of air (V_a) was assumed to be 3%. The water was kept constant at 330 lb per yd^3 (196 kg per m^3) of concrete. This led to a water-to-cement ratio (w/c) of 0.403. This w/c was kept constant throughout the study. The water was selected to get an approximate slump of about 7" (0.180 m) to facilitate easy handling of the rheometer (which can only be used on concrete with a slump greater than 3" (0.075 m)). The control mix had a mortar volume (V_m) of 65% (labeled as mix C). Coarse aggregate made up the rest of the concrete volume.

To study the effect of change in aggregate ratio, four other mixture designs were considered with varied V_m. All the mixtures used in this study are tabulated in Table 2.

Table 2: Volume proportions of concrete mixtures used in this study

Mix ID	Volume (% of total concrete vol.)						% Sand (of total agg., by vol.)
	Paste	Air	Agg.	Mortar	Sand	Coarse agg.	
A	35	3	62	55	20	42	32
B				60	25	37	40
C				65	30	32	48
D				70	35	27	56
E				75	40	22	65

The volume was converted to appropriate mass using the specific gravity of the material and the batch volume, to batch the material prior to mixing.

3.3 Mixing Procedure

A concrete pan mixer (shown in Figure 12) was used for mixing concrete. The mixing procedure was kept the same for all mixes. First, the pan was wetted with water and the excess water was wiped using paper towels. Both fine and coarse aggregates were added to the pan along with half the mix water and mixed for 30 s. The cement was added to the pan next (and a timer was started simultaneously to measure the hydration time). The remaining water was then added to the pan and mixed for 2 minutes. This was followed by a minute of resting period (during which the concrete was manually overturned within the pan using scoops to ensure thorough mixing). The concrete was further mixed for another minute after the rest period. Care was taken to finish the entire process within 5 minutes (3.5 minutes of actual mixing, a minute of rest, and time to add cement and water).

Figure 12: Concrete pan mixer.

3.4 Rheometer Setup

A rheometer developed by the International Center for Aggregate Research (ICAR) was used in this study. The ICAR test setup consists of a bucket to hold concrete, a torque meter and a vane (5” (0.127 m) in height and diameter) for measurement, and a computer to control the torque meter as shown in Figure 13. The torque meter is placed directly on the bucket with the help of a frame, with the vane attached to the torque meter as shown in Figure 14.

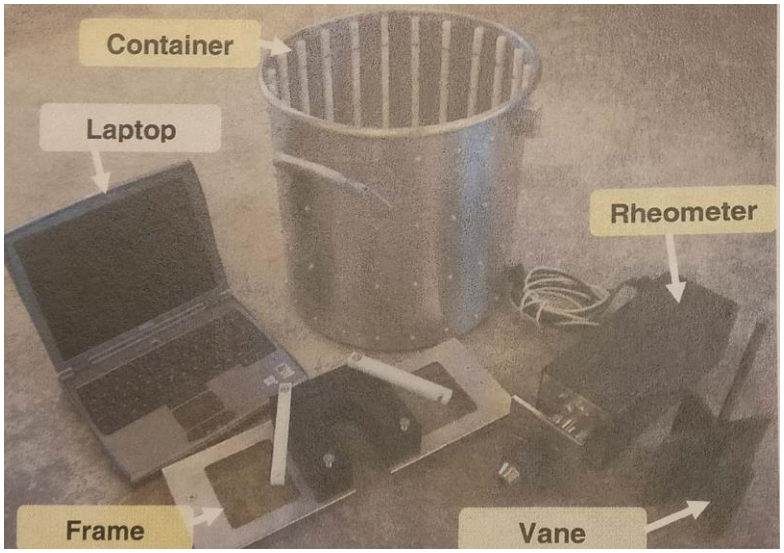

Figure 13: ICAR rheometer components.

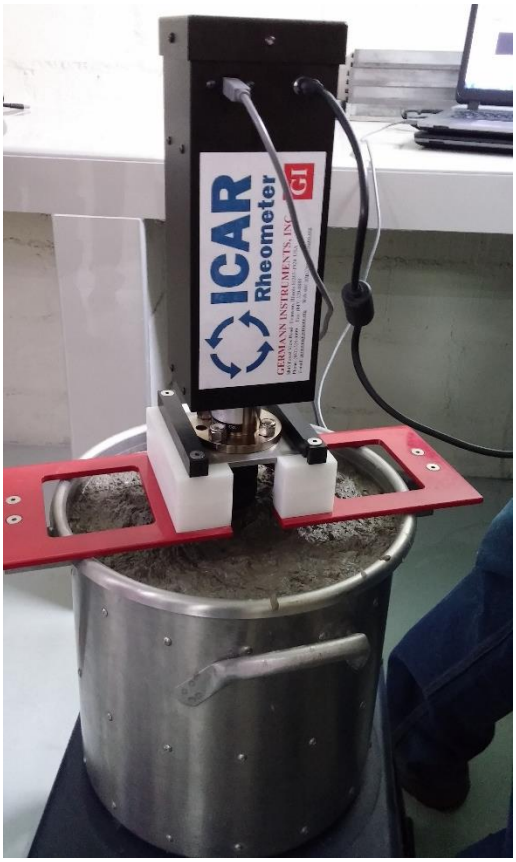

Figure 14: ICAR rheometer setup.

To study the effect of vibration on rheology, the ICAR rheometer was modified. The bucket was placed on a vibration table (frequency of 60 Hz and maximum amplitude of 0.001 m) and the torque meter was placed on a stand to eliminate direct transmission of vibration into the rheometer. The stand was designed such that the torque meter was suspended slightly above the bucket (~ 0.5” (0.01 m)). The modified ICAR rheometer setup is shown in Figure 15. Ratchet clamps were used to ensure the bucket did not move during vibration. During testing, it was always made sure that the bucket was placed at the center of the vibration table and the stand was designed such that the vane was suspended above the center of the vibration table.

Figure 15: Modified ICAR Rheometer setup.

The test procedure was kept constant for all tests since the shear history of the concrete is important. The rheometer bucket was filled with concrete in two layers, each tamped with a tamping rod 25 times, to the top of the vertical strips present in the ICAR bucket. The bucket was then placed on the vibration table and clamped to it using ratchet clamps. The vane was then placed in the concrete by placing the torque meter on the stand. To erase the shear history of the concrete, the vibration table was vibrated at maximum amplitude for 10 seconds, starting 15 seconds before the first stress growth test.

Stress growth test was performed to measure the static yield stress of concrete. This test involved rotating the vane at a constant low shear speed of 0.025 revolutions per second (rps). The torque required to maintain this constant shear speed was monitored over time. The maximum torque corresponds to the static yield stress of the material. Based on the vane geometry and the maximum torque, the ICAR rheometer could compute the static yield stress of the concrete. The equation to compute static yield is given below and it can be seen that the static yield stress is proportional to the torque:

$$\tau_o = \frac{2T}{\pi D^3\left(\frac{H}{D}+\frac{1}{3}\right)} \quad (2)$$

where,

τ_o is the static yield stress;

T is the maximum torque;

D is the diameter of the vane; and

h is the height of the vane.

To evaluate the growth of static yield stress of concrete with time, the stress growth test had to be carried out at various hydration times. Since the stress growth measurement disturbs the concrete, each test required a new batch of concrete. But, in the interest of time and material, it was decided to use the same concrete multiple times. Different time intervals between measurements were evaluated to find an optimum time interval to allow the rebuilding of the cement paste microstructure. Intervals of 5, 10 and 15 minutes were evaluated.

Once an optimum time interval (5 min.) was decided (refer to Chapter 4 – Results and Discussion), a testing protocol was determined. While determining the protocol, the end application of concrete 3DP was considered. The printing process usually takes place 15 to 60 minutes after mixing concrete (Stynoski, P., personal communication, April 2018). The test protocol is tabulated in Table 3. The vibration was always at the maximum amplitude of the vibration table unless specified otherwise.

Step 9 in the test protocol begins a loop which goes back to step 3 (starting at 22 min. and continuing at the same time intervals). The 7-minute rest and vibration period between steps 2 and 9 were repeated multiple times to study the effects of vibration on the yield stress of concrete at various hydration times. Each loop represents the deposition of a layer of concrete during concrete 3DP.

Table 3: Modified ICAR testing protocol

Step	Hydration time	Action	Remarks
1	14 min. 45 s	Vibration switched on to clear shear history	Mimics initial vibration in concrete 3DP
2	14 min. 55 s	Vibration turned off	Mimics concrete exiting the vibrating nozzle of the 3D printer
3	15 min.	Start stress growth test on ICAR rheometer	Measures static yield stress
4	20 min.	Start stress growth test on ICAR rheometer	Measures static yield stress gained to sustain the weight of the next printed layer.
5	20 min. 30 s	Vibration turned on; start stress growth test	Measures yield stress during vibration
6	21 min.	Start stress growth test	Measures yield stress during vibration
7	21 min. 30 s	Start stress growth test	Measures yield stress during vibration
8	21 min. 55 s	Stop vibration	55 s mimics the conditions set by the initial shear history clearing vibration
9	22 min.	Start stress growth test on ICAR rheometer	Measures static yield stress

CHAPTER 4: RESULTS AND DISCUSSIONS

The results from the experiments carried out are presented and discussed in this chapter.

4.1 Determining Optimum Measurement Interval

Ideally, to plot the increase in yield stress of concrete with time, each measurement must be done on a new sample. Since this would require a considerable amount of time and material, it was investigated if a longer time interval between measurements would allow sufficient time for the thixotropic build up. Three different time intervals were investigated. The results from the tests are shown in Figure 16. Mix C was used in each case.

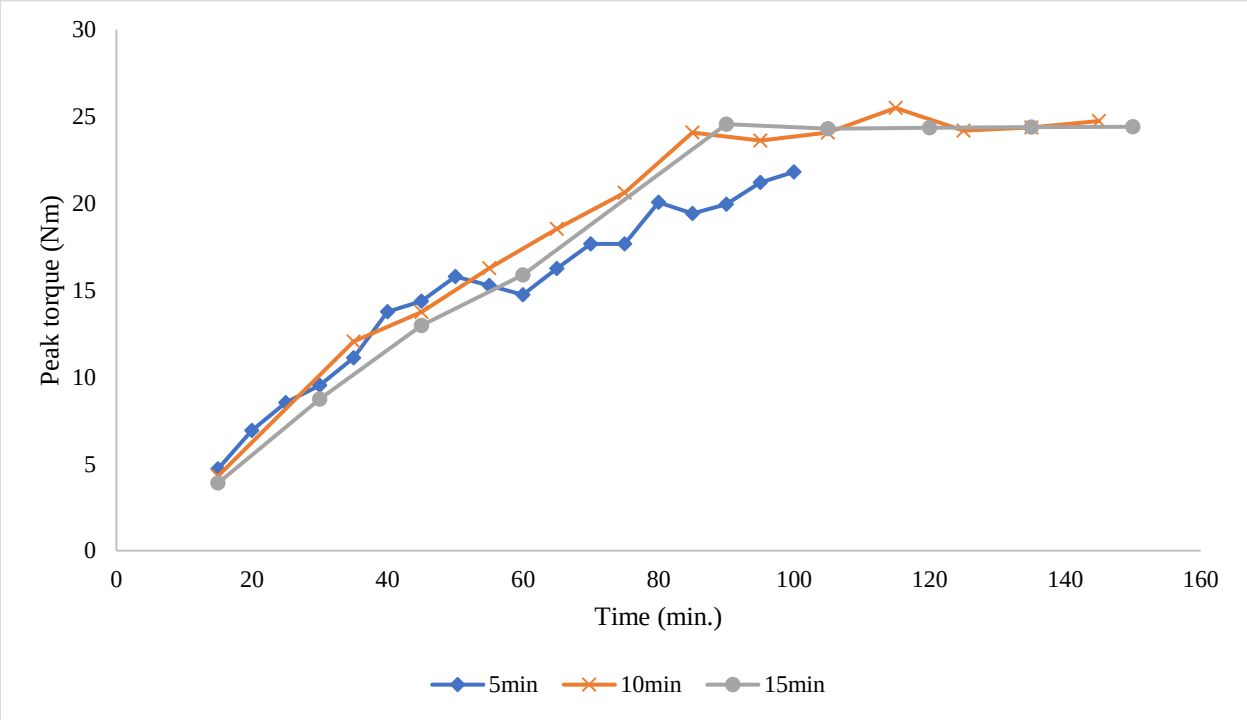

Figure 16: Peak torque versus time for different measurement intervals.

It was observed that the measurement time interval made no difference to the yield stress growth with time. A possible explanation for this can be provided by considering the source of yield stress in concrete. The yield stress in concrete originates from three different sources; time-dependent thixotropy (flocculation at rest and deflocculation under shear), the structural build-up of cement paste and frictional stress between aggregates. With the increase in hydration time, the ongoing chemical reactions cause yield stress to increase with the formation of irreversible additional hydrates that cause better cohesion of the flocculated structure [21]. The contribution of aggregates towards the yield stress (frictional stress due to interlock) does not change with time and is dependent only on the orientation with each other which can be assumed to remain the same. The structural breakdown of cement paste is irreversible and hence plays no role in the yield stress growth when the same sample is sheared multiple times [16]. Thus, thixotropy is the reason for the increase in yield stress of concrete with time in this scenario. The measurement interval is thus governed by the rate of flocculation at rest. Since the plot of torque versus time for all the three considered time intervals are identical (some variations to be expected as the ICAR rheometer has a coefficient of variation (COV) of 10%), it was concluded that 5 minutes of rest between measurements was greater than the time required for complete re-flocculation of the suspended particles in the disturbed cement paste.

The measurement time interval of five minutes between successive measurements was considered as the optimum since this would allow a greater number of data points to be collected. Also, considering concrete 3DP, this was assumed to be the minimum time that would be required for the nozzle to come back to a given spot after printing a layer.

It should be noted that the ICAR rheometer can only measure torque up to 24 Nm accurately. This instrument limitation led to incorrect data to be recorded beyond 90 minutes.

4.2 Reliability of the Modified ICAR Rheometer

Since the rheometer was modified and was being used in a geometry and condition different to the way it was intended to be used, its performance was assessed. The ICAR rheometer has a COV of 10%. This has been attributed mainly to shear history and material variance by the developers of the rheometer [24]. The same concrete mixture design was tested in the same way three different times and the results are plotted in Figure 17.

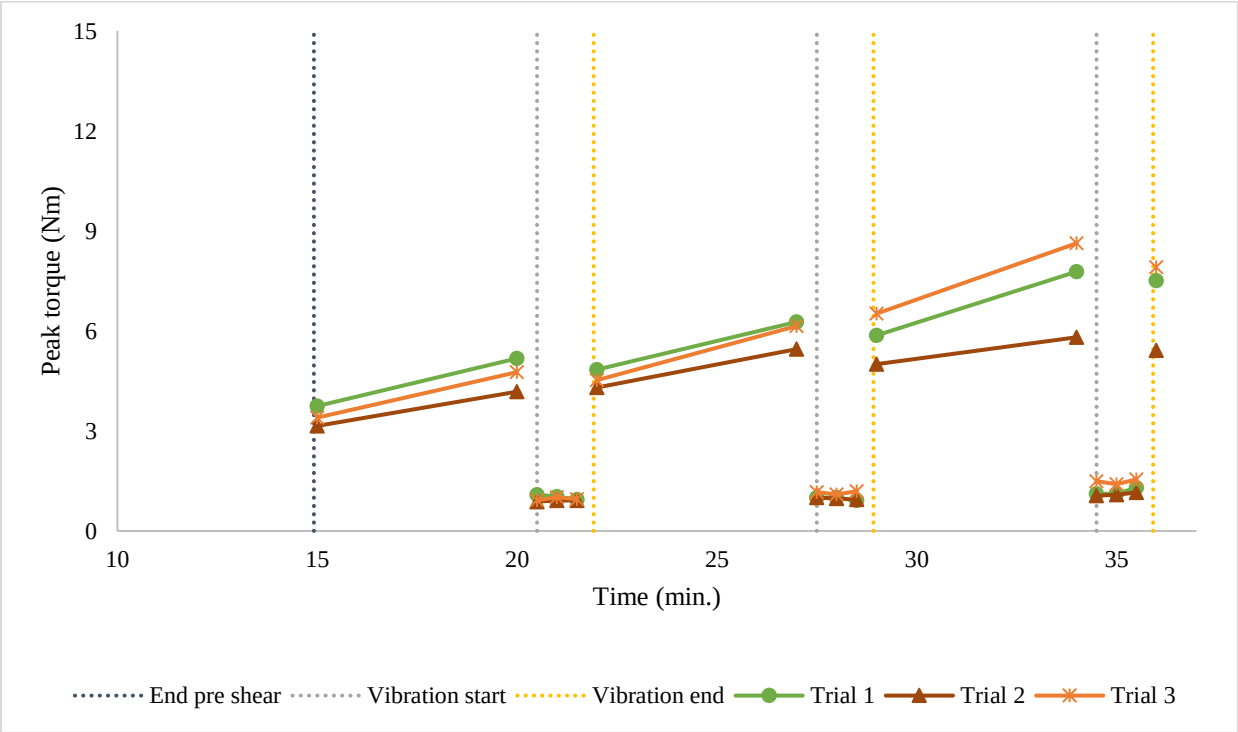

Figure 17: Peak torque versus time from the modified ICAR rheometer repeatability test.

The average COV for all the measured values of torque was found to be 11.5%. The greater COV was expected since the ICAR rheometer was not designed to be used during vibration. For the qualitative study being conducted, this was deemed to be acceptable.

The effect of varying sand content on the yield stress of concrete has been established in the literature [27]. Tests were conducted with the modified ICAR rheometer to verify if similar results could be obtained. Mixture designs A, B, C, D, and E were tested under the testing protocol established (Table 3) and the results are plotted in Figure 18. The variation of peak torque with sand content is plotted in Figure 19.

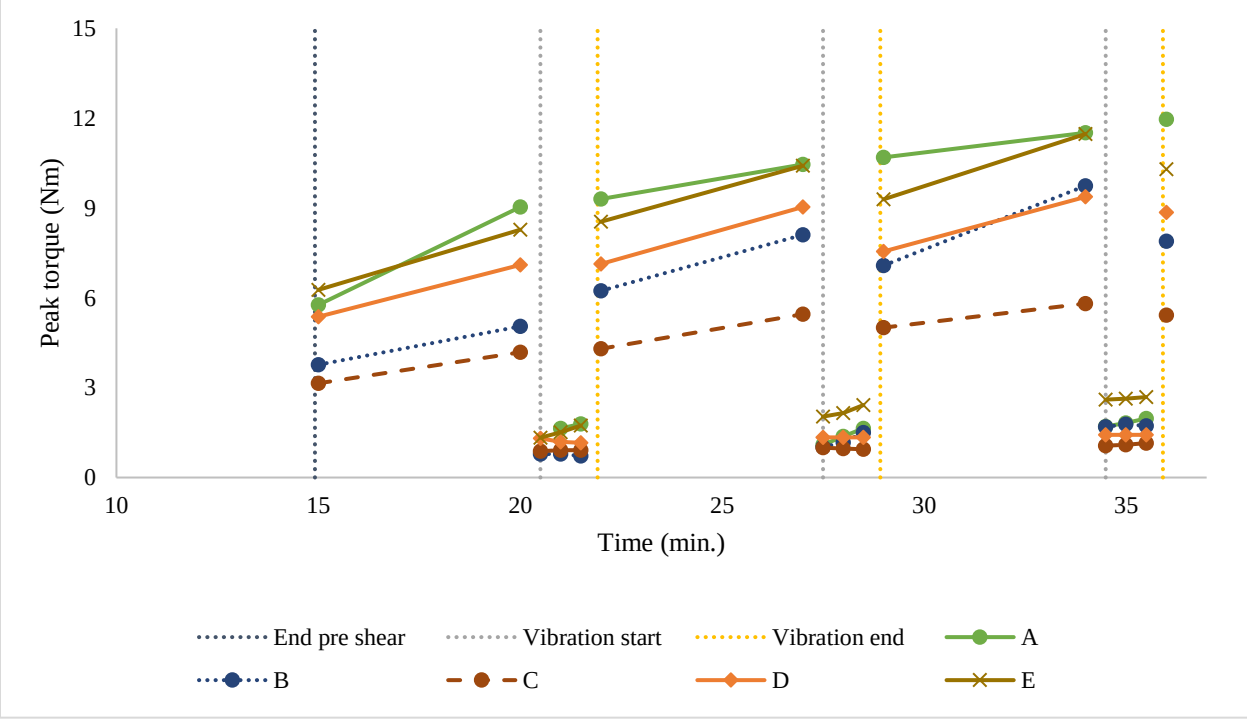

Figure 18: Peak torque versus time for varied sand content.

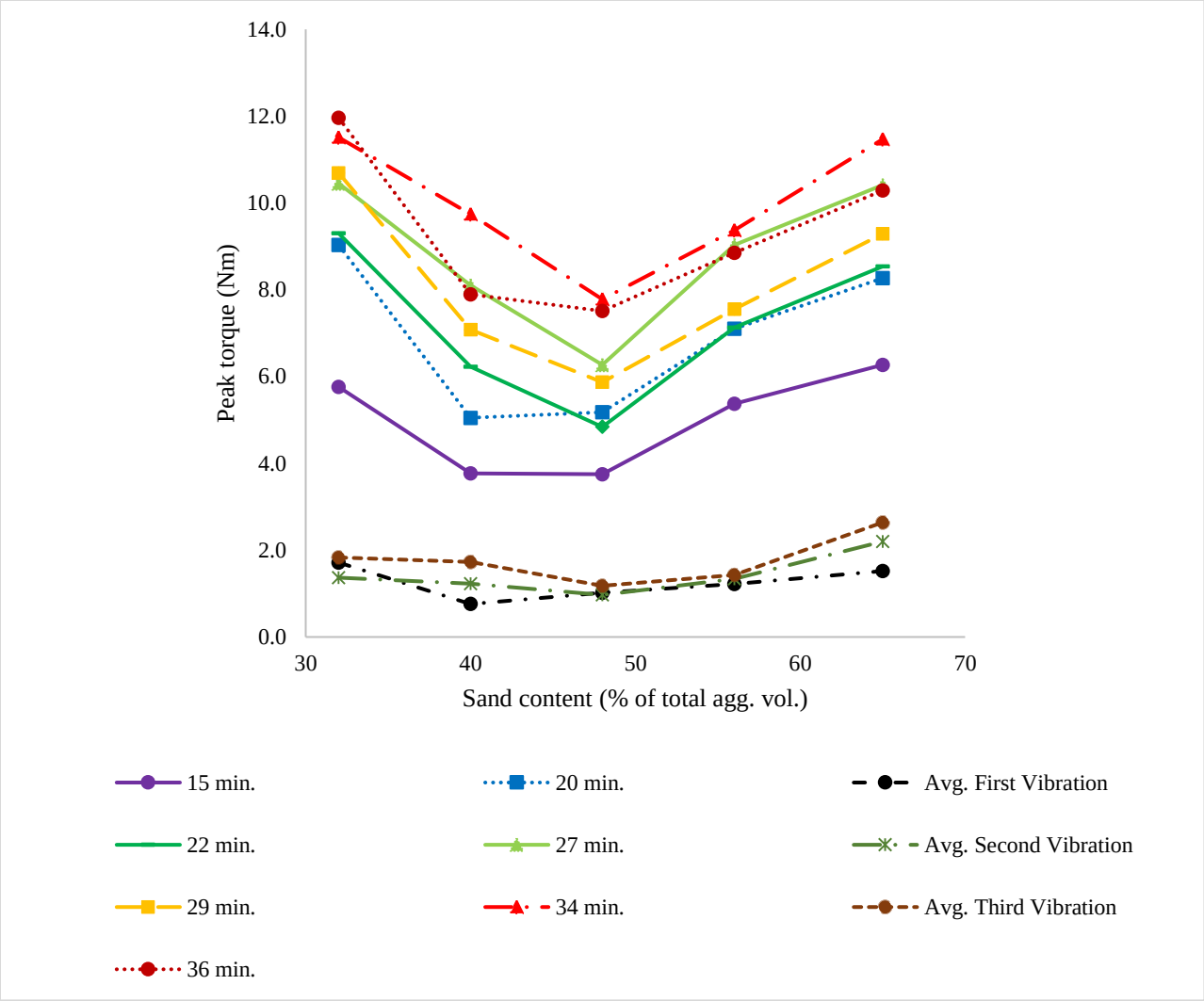

Figure 19: Peak torque versus sand content at various hydration time.

The parabolic relationship between yield stress and sand content was observed at all hydration ages, with minimum yield stress observed at the intermediate sand content (40 to 48% of total aggregate by volume) as expected [27]. The modified ICAR rheometer could repeat experimental data from the literature.

It was observed from the results of this test (Figures 18 and 19) that the torque measured 5 seconds after vibration was turned off is slightly lower than the torque measured immediately before the

vibration (an average loss of 8% torque) for the second and third vibration. The literature claims that the effect of vibration is instantaneously and completely recovered but this was not observed [16]. This loss in yield stress could be due to several reasons; the modified ICAR rheometer's inability to capture slight variations accurately (COV = 11.5%), aggregate settlement due to the geometry of the rheometer setup, and/or thixotropic buildup requiring more than 5 seconds. Additional work needs to be carried out to determine the reason accurately.

However, for the first vibration, there was an average increase in yield stress (5% increase in torque) after vibration compared to the pre-vibration yield stress. This could potentially be explained by the fact that the cement hydration occurs at a rapid pace in the first stage of its hydration before the dormant period begins. It is possible that the structural build-up of cement paste outpaces the irreversible structural breakdown occurring due to the vibratory shear stresses. Further research is required to ascertain this reasoning.

Since the volume of paste was constant between all the concrete mixtures, at high sand content, due to the greater surface area of aggregates, more paste was required to coat the aggregates completely to reduce friction and the general lack of excess paste increases the yield stress. At low sand content, the higher proportion of (angular) coarse aggregate causes higher frictional stresses and causes the greater yields stress.

The measurements acquired during a vibration period were all comparable for a given mixture design. Because of this, no noise correction was carried out to data obtained during vibration (despite separating the torque meter from the vibration table, some vibration was still picked up by it).

4.3 Effect of Vibration on Yield Stress Growth

Concrete 3DP of full-scale structures will require a considerable amount of printing time. To hasten the printing process, a possible solution would be to mix a large quantity of concrete and print it without any stoppages for loading the printer with fresh concrete. In the current extrusion based concrete 3DP, the printing time is limited by the fact that cementitious material gains yield stress with time and cannot be extruded beyond a certain time period. However, with the use of vibration, there is potential for a longer window in which concrete could be 'printed'. To investigate this, concrete (Mix C) was subjected to the test protocol for up to 150 minutes after the start of hydration. The cement used was known to have a setting time of about 120 minutes. The results from this test are shown in Figure 20 (and similar results are also shown in APPENDIX B).

It was observed that the yield stress during vibration of concrete dropped considerably throughout the dormant period. The drop in the value of torque with vibration and gain after it was turned off was instantaneous as noted in the literature.

Vibration caused a delay in the overall yield stress growth in concrete. When compared to concrete which was not vibrated, and static yield stress measured every 15 minutes, vibration had caused a slower growth of yield stress. Thixotropic rebuilding depends on the shear history and is a possible explanation for this. This could potentially help in concrete 3DP as (continuous) vibration of the concrete in the reservoir of the printer will slow down the rate of slump loss and help create a longer window for printing. Since the response of concrete to vibration mostly remains the same throughout its dormant period, by using retarders, a longer dormant period can help create a longer window for printing.

Beyond 120 minutes, the rate of gain of yield stress in the five-minute rest period was significantly greater than during the dormant period. This was a clear sign of the end of the dormant period and the beginning of the acceleration period in cement hydration (initial set).

To compare the effect of vibration amplitude on yield stress growth, the vibration table was used at ‘half’ setting and the results are plotted in Figure 21 (the vibration table used did not have a well-defined control mechanism to alter the amplitude of vibration). The level to which the yield stress decreases during vibration reduced considerably when compared to maximum amplitude vibration. Further testing is necessary to quantify the effects of vibration amplitude. The maximum amplitude used in this study was a limitation of the vibration table. The effect of a greater amplitude needs to be evaluated.

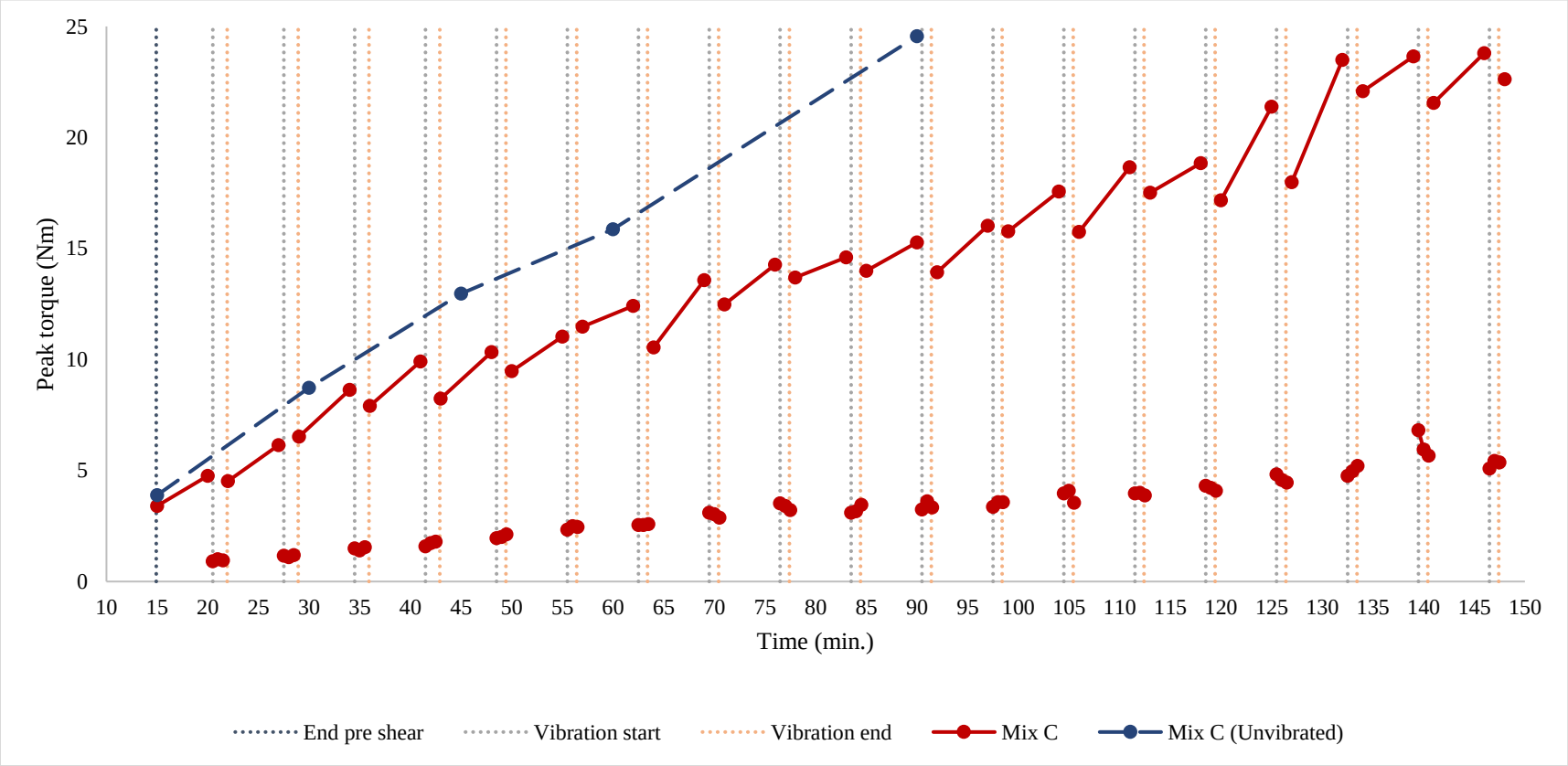

Figure 20: Peak torque versus time over the entire dormant period of concrete.

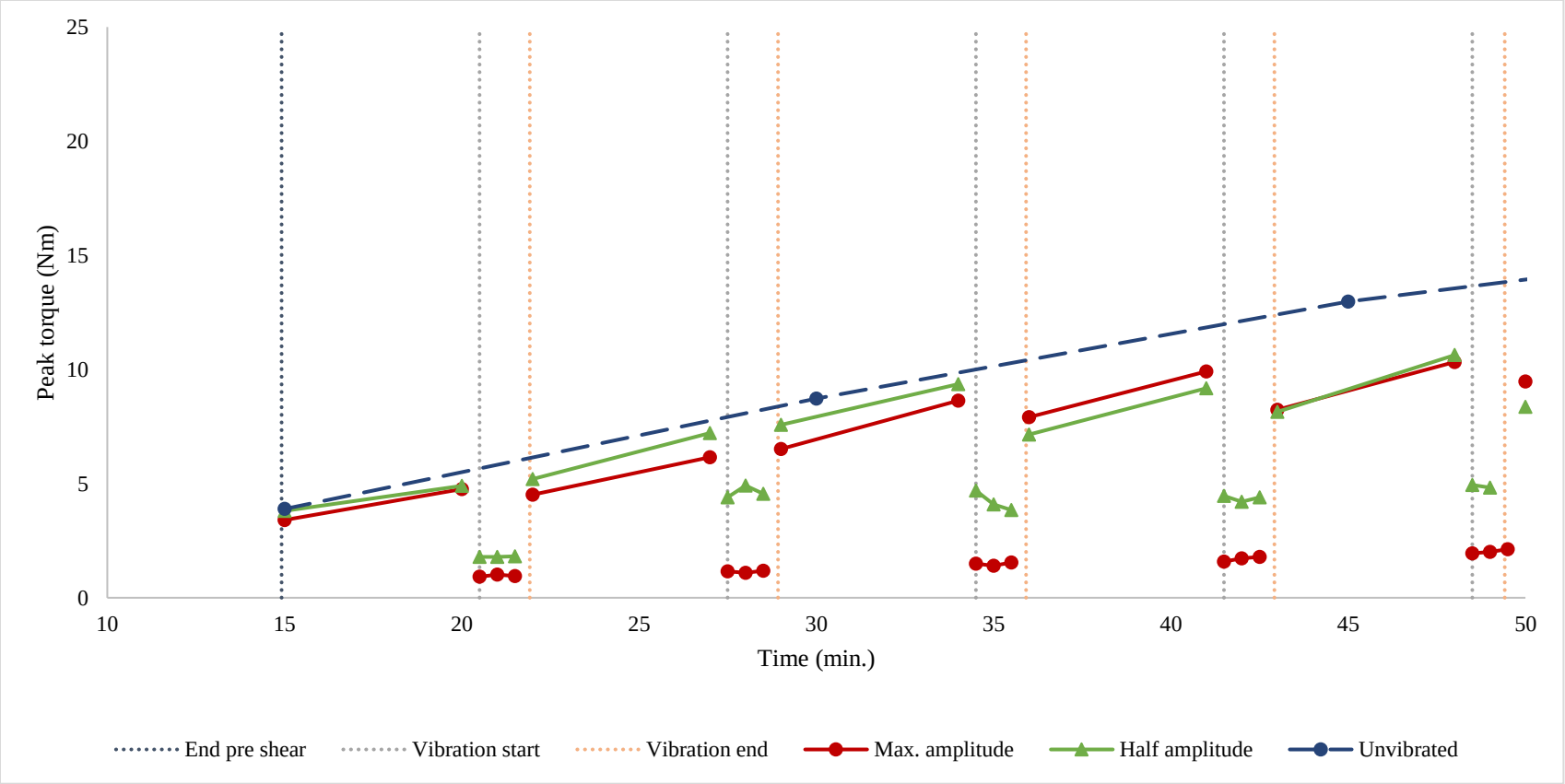

Figure 21: Peak torque versus time for different vibration amplitude.

CHAPTER 5: CONCLUSIONS

This research developed an experimental protocol to measure yield stress during vibration that also mimicked the concrete 3DP process. Various quantitative studies need to be carried out to further the work presented here and has been discussed in relevant places.

Further, based on the review of the literature and experimental work carried out as a part of this research project, the following conclusions are drawn:

- Stress growth measurements can be repeatedly carried out on the same concrete sample if there is a sufficient rest period between measurements.
- An ICAR rheometer can be modified to operate reliably during vibration.
- A parabolic relationship between yield stress and sand content exists and this was verified at various hydration ages.
- Vibration causes the yield stress growth to occur at a slower pace in concrete compared to concrete which is not vibrated.
- The effect of vibration on concrete is immediate and reversible throughout the dormant period of the concrete.
- The effect of vibration on concrete is dependent on the amplitude of vibration.

REFERENCES

[1] T. S. Rushing *et al.*, "Investigation of concrete mixtures for additive construction," *Rapid Prototype J.*, vol. 23, no. 1, pp. 74–80, 2017.

[2] T. Di Carlo, B. Khoshnevis, and Y. Chen, "Manufacturing Additively, With Fresh Concrete," in *ASME International Mechanical Engineering Congress and Exposition, Volume 2A: Advanced Manufacturing*, 2013, p. V02AT02A007.

[3] B. Khoshnevis, "Automated construction by contour crafting—related robotics and information technologies," *Autom. Constr.*, vol. 13, no. 1, pp. 5–19, Jan. 2004.

[4] S. Lim, R. A. Buswell, T. T. Le, S. A. Austin, A. G. F. Gibb, and T. Thorpe, "Developments in construction-scale additive manufacturing processes," *Autom. Constr.*, vol. 21, pp. 262–268, 2012.

[5] "Thai Cement Producer SCG Uses Delta WASP 3D Printer for Architectural Projects - 3Printr.com." [Online]. Available: https://www.3printr.com/thai-cement-producer-scg-uses-delta-wasp-3d-printer-architectural-projects-5739123/. [Accessed: 07-Jul-2018].

[6] M. Jazdyk, "3-D printing a building," *Press Release*. [Online]. Available: https://www.usace.army.mil/Media/News-Archive/Story-Article-View/Article/1288744/3-d-printing-a-building/. [Accessed: 07-Jul-2018].

[7] "DuBox to showcase the first 3D printed concrete element in UAE." [Online]. Available: http://www.dubox.me/dubox-showcase-first-3d-printed-concrete-element-uae/. [Accessed: 07-Jul-2018].

[8] "First On-Site House has Been 3D-Printed by Apis Cor in 24 Hours | Digital Trends." [Online]. Available: https://www.digitaltrends.com/home/apis-cor-3d-printed-house/.

[Accessed: 07-Jul-2018].

[9] B. Zareiyan and B. Khoshnevis, “Effects of mixture ingredients on interlayer adhesion of concrete in Contour Crafting,” *Rapid Prototype J.*, vol. 24, no. 3, pp. 584–592, Apr. 2018.

[10] A. Kazemian, X. Yuan, E. Cochran, and B. Khoshnevis, “Cementitious materials for construction-scale 3D printing: Laboratory testing of fresh printing mixture,” *Constr. Build. Mater.*, vol. 145, pp. 639–647, Aug. 2017.

[11] B. Zareiyan and B. Khoshnevis, “Effects of interlocking on interlayer adhesion and strength of structures in 3D printing of concrete,” *Autom. Constr.*, vol. 83, pp. 212–221, Nov. 2017.

[12] T. T. Le *et al.*, “Hardened properties of high-performance printing concrete,” *Cem. Concr. Res.*, vol. 42, no. 3, pp. 558–566, 2012.

[13] T. T. Le, S. A. Austin, S. Lim, R. A. Buswell, A. G. F. Gibb, and T. Thorpe, “Mix design and fresh properties for high-performance printing concrete,” *Mater. Struct.*, vol. 45, no. 8, pp. 1221–1232, Aug. 2012.

[14] A. Kazemian, X. Yuan, R. Meier, E. Cochran, and B. Khoshnevis, “Construction-Scale 3D Printing: Shape Stability of Fresh Printing Concrete,” in *ASME. International Manufacturing Science and Engineering Conference, Volume 2: Additive Manufacturing; Materials*, 2017, p. V002T01A011.

[15] A. Perrot, D. Rangeard, and A. Pierre, “Structural built-up of cement-based materials used for 3D-printing extrusion techniques,” *Mater. Struct. Constr.*, vol. 49, no. 4, pp. 1213–1220, 2016.

[16] G. H. Tattersall and P. H. Baker, “The effect of vibration on the rheological properties of fresh concrete,” *Mag. Concr. Res.*, vol. 40, no. 143, pp. 79–89, Jun. 1988.

[17] S. Juradin and P. Krstulovic, “The vibration rheometer: The effect of vibration on fresh concrete and similar materials,” *Materwiss. Werksttech.*, vol. 43, no. 8, pp. 733–742, 2012.

[18] G. H. Tattersall and P. H. Baker, “An investigation on the effect of vibration on the workability of fresh concrete using a vertical pipe apparatus,” *Mag. Concr. Res.*, vol. 41, no. 146, pp. 3–9, Mar. 1989.

[19] J. A. Koch, “Shaking, slamming, and vibrating yield-stress fluids: inducing particle motion in rheologically-complex materials,” University of Illinois, 2017.

[20] S. Mindess, J. F. Young, and D. Darwin, *Concrete*, 2nd ed. Prentice Hall, 2003.

[21] P.-C. Aïtcin and R. J. Flatt, Eds., *Science and technology of concrete admixtures*. Woodhead Publishing, 2016.

[22] “ASTM C143 / C143M-15a, Standard Test Method for Slump of Hydraulic-Cement Concrete.” ASTM International, West Conshohocken, PA, www.astm.org, 2015.

[23] N. Roussel, “Correlation between Yield Stress and Slump: Comparison between Numerical Simulations and Concrete Rheometers Results,” *Mater. Struct.*, vol. 39, no. 4, pp. 501–509, Aug. 2007.

[24] E. Koehler and D. Fowler, “Development of a Portable Rheometer for Fresh Portland Cement Concrete,” Austin, TX, 2004.

[25] B. S. Choo and J. (John B. Newman, Eds., *Advanced concrete technology 2: Concrete properties*. Butterworth-Heinemann, 2003.

[26] O. H. Wallevik and J. E. Wallevik, “Rheology as a tool in concrete science: The use of rheographs and workability boxes,” *Cem. Concr. Res.*, vol. 41, no. 12, pp. 1279–1288, Dec. 2011.

[27] R. S. Szecsy, “Concrete Rheology,” University of Illinois, 1997.

[28] P. F. G. Banfill, British Society of Rheology., and E. International Conference on Rheology of Fresh Cement and Concrete (1990 : Liverpool, *Rheology of fresh cement and concrete : proceedings of the international conference organized by the British Society of Rheology, University of Liverpool, UK, March 26-29, 1990*, 1st ed. E. & F.N. Spon, 1991.

[29] “ASTM C150 / C150M-18, Standard Specification for Portland Cement.” ASTM International, West Conshohocken, PA, 2018, www.astm.org.

[30] “ASTM C127-15, Standard Test Method for Relative Density (Specific Gravity) and Absorption of Coarse Aggregate.” ASTM International, West Conshohocken, PA, 2015, www.astm.org.

[31] “ASTM C128-15 Standard Test Method for Relative Density (Specific Gravity) and Absorption of Fine Aggregate.” ASTM International, West Conshohocken, PA, 2015, www.astm.org.

[32] “ASTM C136 / C136M-14, Standard Test Method for Sieve Analysis of Fine and Coarse Aggregates.” ASTM International, West Conshohocken, PA, 2014, www.astm.org.

APPENDIX A: ICAR RHEOMETER SAMPLE RAW DATA

The ICAR rheometer measures the torque required to maintain the shear speed set for a shear growth test. The raw data from this test is a plot of torque (in Nm) versus time (in s). The peak torque from this plot is selected to calculate yield stress. A sample graph of raw data from shear growth test is shown in Figure 22 and a sample graph of data from a shear growth test during vibration is shown in Figure 23.

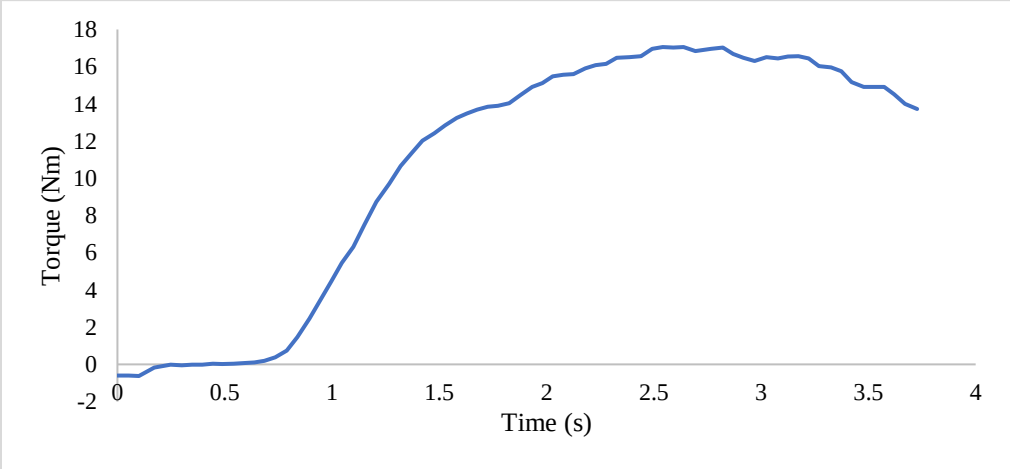

Figure 22: Torque versus time: sample raw data - ICAR shear growth test.

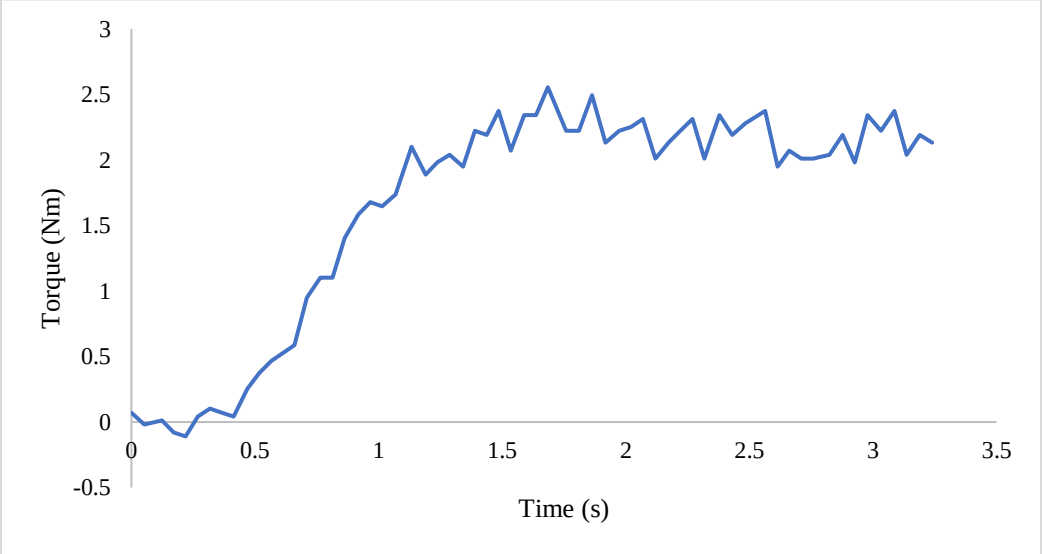

Figure 23: Torque versus time: sample raw data - ICAR shear growth test during vibration.

APPENDIX B: REPEATABILITY OF EXPERIMENTAL DATA

The test to study the effect of vibration on the yield stress over the dormant period of concrete (as discussed previously in section 4.3 and shown in Figure 20) was repeated to see if the results could be replicated. The results from this repeated test are shown in Figure 24. A similar test was also carried out during the development stage of the test protocol and the results from that test are also included in Figure 24 below. It is to be noted that the test during the development stage had a lower vibration amplitude and a different time schedule for vibration. However, the data are plotted and shown together since the qualitative behavior is similar.

When repeated, the data from this test showed repeatability, especially during vibration.

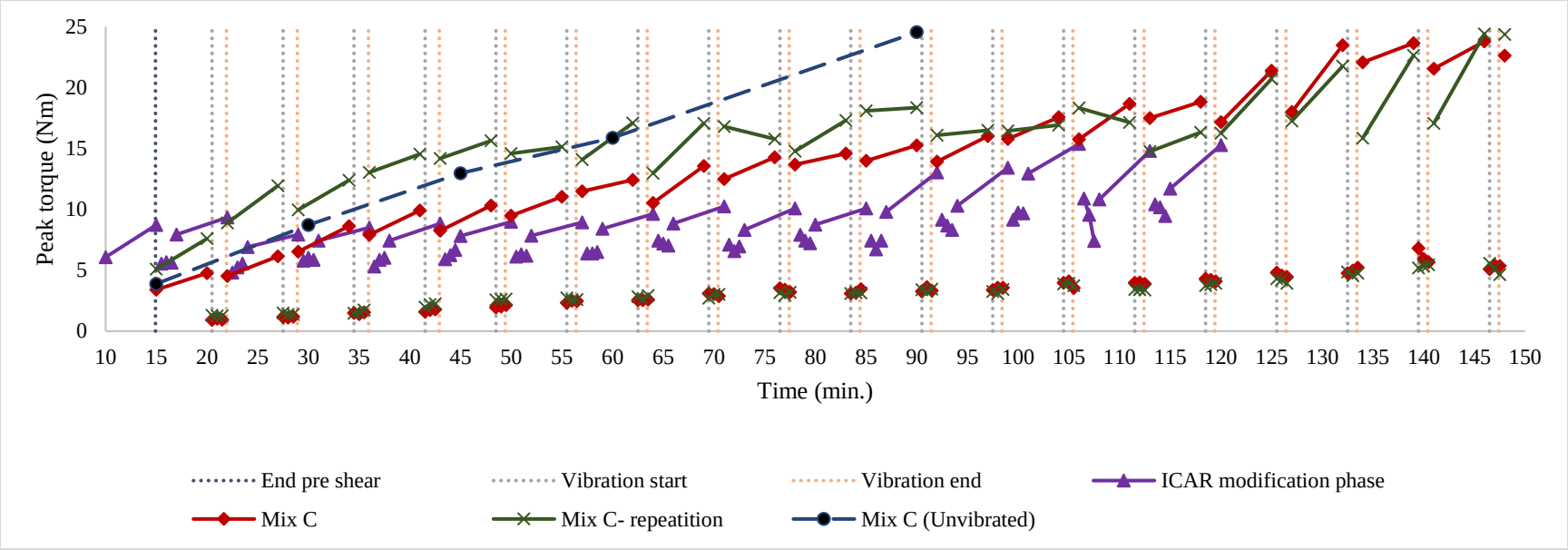

Figure 24: Repeatability of peak torque versus time over the entire dormant period of concrete.

APPENDIX C: MODIFICATION OF THE ICAR RHEOMETER AND DEVELOPMENT OF THE TEST PROTOCOL

During the ICAR rheometer setup modification stage, to test if the modification affected the ICAR rheometer's ability to collect good data, its measurements were compared with another ICAR rheometer in its original set up. The same concrete mixture was tested simultaneously and the results from this test are shown below in Figure 25. The test was repeated (results are shown in Figure 26), and in both trials, the modified ICAR displayed similar trends as the original ICAR but with a lower peak torque.

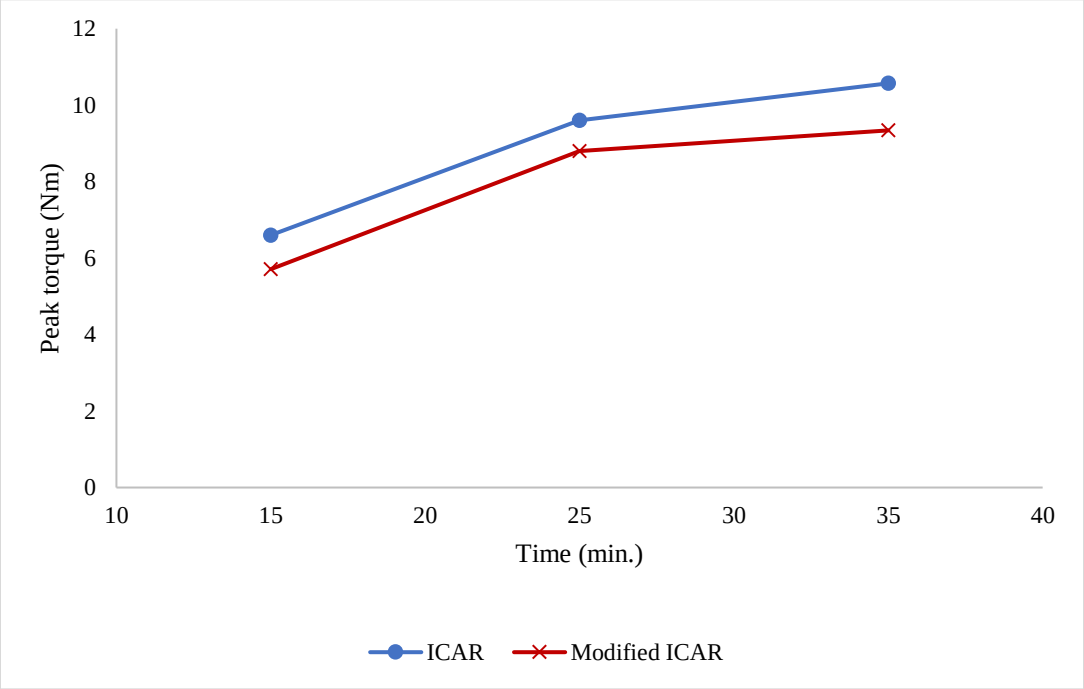

Figure 25: Comparing ICAR rheometer with modified ICAR rheometer.

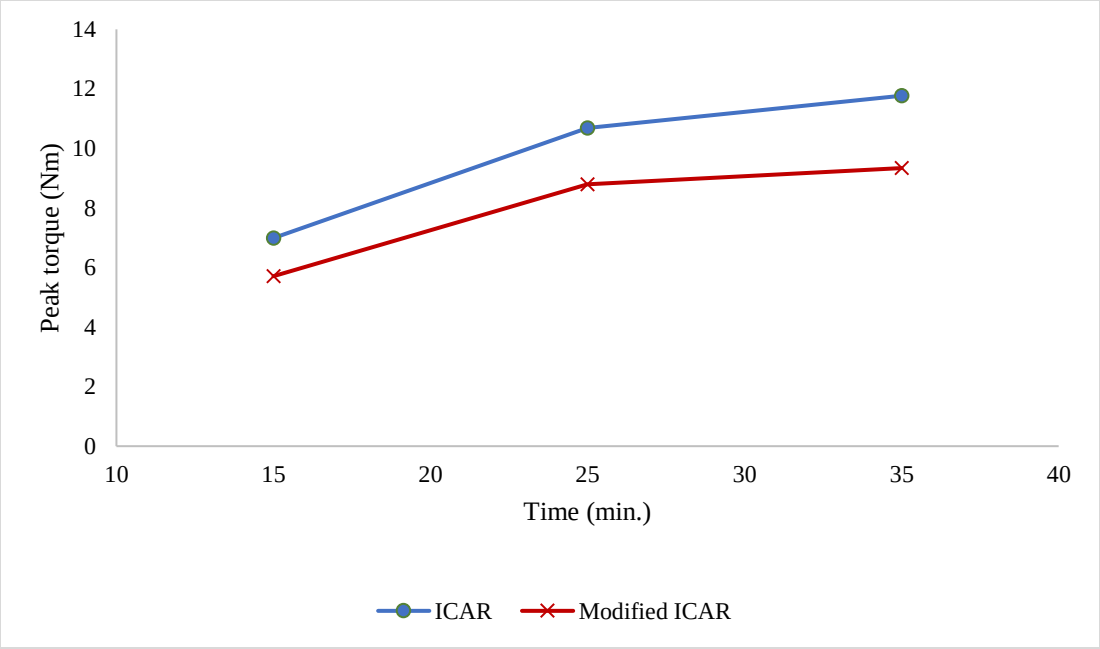

Figure 26: Comparing ICAR rheometer with modified ICAR rheometer (repeated test results).

Initially, step 1 of the test protocol started at 9 min. 45 s instead of the 14 min. 45 s which was adopted in the final protocol. The change was made mainly because it was not a realistic time to start concrete 3DP. The actual process of mixing concrete and loading it in to the reservoir of the concrete 3D printer and initiating the printing process was envisioned to take longer than 10 minutes. This was also backed by the advice of Dr. Stynoski (US army CERL). His experience with concrete 3DP suggested it takes anywhere between 15 min. to 60 min. after mixing to start printing due to various practical issues that come up while printing large-scale structures. Some results from this earlier test protocol is shown in Figure 27. It can be observed that the torque recorded after vibration is higher than the pre-vibration torque. This could be because of the rapid hydration reaction during the initial 20 min. (Stage 1 of hydration reaction) or presence of ettringite.

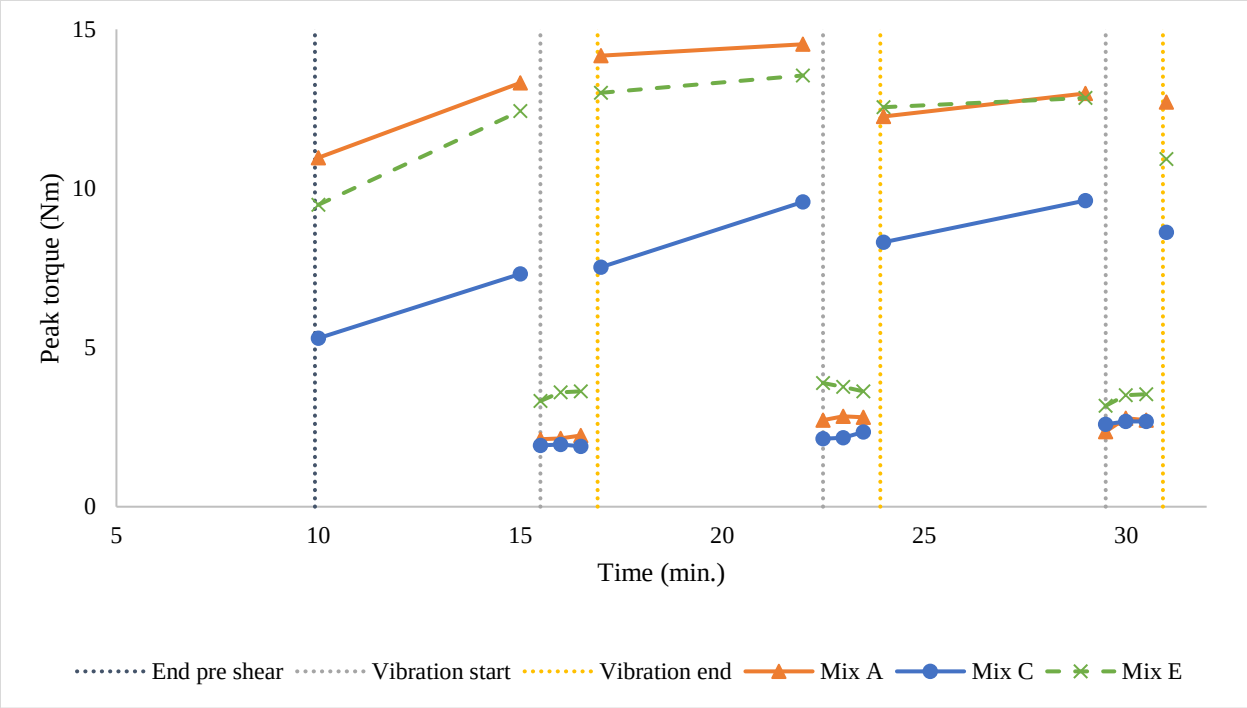

Figure 27: Peak torque versus time for varied sand content.

The parabolic relationship of sand content and yield stress is seen in these experimental results too. Mixes B and D were developed later to determine the sand content at which the vertex of the parabola occurred.